ChemPubSoc Europe

DOI: 10.1002/open.201900065

Open Access ChemistryOPEN Full Papers

Facile Preparation and Properties of Crosslinked Copolyether Elastomers with 1,2,3-Triazole and Urethane Subunit via Click Polymerization

Qian Zhang,[a, b] Ning Liu,[b] Hongchang Mo,[b] Xianming Lu,[b] Yao Wang,[c] Minghui Xu,[b] and Yuanjie Shu*[a, b]

An azide terminated ethylene oxide-tetrahydrofuran copolymer with urethane segments (ATUPET) as a novel binder prepolymer, has been prepared through ethylene oxide-tetrahydrofuran random copolymer (PET) end-capping modification via one-pot method. The structure characterization of the modifier has been analyzed by FTIR, ^{1}H NMR, ^{13}C NMR and GPC. In comparison with PET, ATUPET has a slightly higher viscosity because it has additional hydrogen bonding interaction generated by the urethane in ATUPET. Triazole cross-linked elastomers based on ATUPET with various functional molar ratios were prepared using tripropargylamine as a curing agent and cross-linker. Mechanical properties indicate that the modulus E and tensile strength σ_b exhibit a parabolic dependence with the increase in R. At around the stoichiometric ratio, the modulus E and tensile strength σ_b reach a maximum and the elongation at break exhibit an acceptable value at the same time. Swelling tests demonstrate that the apparent cross-linking densities (N_0) have a maximum value at the stoichiometric ratio. Thermal analysis shows that the ATUPET prepolymer and its polytriazoles elastomers exhibit a satisfactory stability. The results demonstrated that ATUPET might be a promising polymeric binder for future propellant formulations especially in the field of isocyanate-free curing technology.

1. Introduction

Cross-linked polyurethanes, a famous polymer material in the family of elastomers, have a significant application in propellants by the virtue of high abrasion, chemical resistance, low-temperature-controlled cure and excellent mechanical properties.[1] On the one hand, they can act as fuel during combustion for their hydrocarbon backbone. On the other hand, they can perform the binding matrix with the dual role of imparting required dimensional stability to the composite and providing structural integrity and good mechanical properties to propellant.[2] Generally, cross-linked polyurethane binder systems are formed by the polyaddition reaction of hydroxyl-terminated pre-polymers and polyfunctional isocyanates. However, these well-known polyurethane binders could undergo side reactions (e.g., the humidity sensitivity of curing process, leading to degradation of the mechanical properties of propellant) during preparation, storage and application. Additionally, the underlying poor compatibility[3] of isocyanates with energetic oxidizers like ammonium dinitramide (ADN) and hydrazinium nitroformate (HNF) also warrants new cure methodologies for processing high energy propellants.

Many methodologies had been used to realize isocyanate-free curing process. Generally, terminal carboxyl polymers[4] could be cured by epoxy or aziridine curing agents, while terminal epoxy polymers[5] could be cured by amine curing agents. Nevertheless, some drawbacks like the side esterification reactions, the self-polymerizations, the influence of H_2O and the poor compatibility in these systerms will hinder their further applications in CSPs. Therefore, click chemistry[6] as an interlocking reaction pattern has attracted many researchers' attentions. For example, Diels-Alder reaction as a reversible reaction for constructing the self-healing[7] or phase change[8] materials has been extensively investigated. However, as far as we know, the application of the DA reaction in CSPs has not been reported. Comparatively, 1,3-dipolar cycloaddition reaction of an organic azide with an alkyne (Huisgen reaction) yielding triazoles is an alternative and versatile method for realizing cross-linked networks in CSPs.[6,9] Furthermore, this reaction provide a new appealing methodology for binder curing in propellant field because of its merits such as high efficiency, substrate or environmental insensitivity, regioselectivity, mild reaction conditions and good compatibility.[10] There have been many literatures on azide-alkyne reactions for cross-linking binder system based on Glycidyl azide polymer (GAP)[3b,11] and Poly-(3-azidomethyl-3-methyloxetane) (PAMMO).[12] However, the mechanical properties of muti-azide groups binders (GAP or PAMMO) based polytriazoles were unsatisfactory mainly due to the intramolecular wasted loops. Therefore, interpenetrating polymernetwork (IPN), especially

[a] Dr. Q. Zhang, Prof. Y. Shu
Xi'an Modern Chemistry Research Institute, Xi'an, China
E-mail: Syj1204172675@163.com
[b] Dr. Q. Zhang, Dr. N. Liu, H. Mo, Dr. X. Lu, Dr. M. Xu, Prof. Y. Shu
State Key Laboratory of Fluorine and Nitrogen Chemicals, Xi'an, China
[c] Y. Wang
China Tobacco Shaanxi Industrial Co., Ltd., Baoji, China

Supporting information for this article is available on the WWW under https://doi.org/10.1002/open.201900065

the muti-walled carbon nanotubes (MWCNTs) enhanced IPNs,[13] has been investigated to improve GAP based polytriazoles. Additionally, nitrogen-rich hyperbranched polymer based polytriazoles[14] also has been reported and may improve the energetic properties of propellants. However, the controllable polytriazoles network based on terminal functional telechelic polymer (Hydroxyl terminated polybutadiene (HTPB)[2,15] and Polycaprolactone ether (PCE)[3c,16]) still be a hot research field. Furthermore, hydroxyl terminated polyether as important binder pre-polymers applied in Nitrate Ester Plasticized Polymer (NEPE) propellant is also necessary to be used to build polytriazoles cross-linking networks via 1,3-Dipolar cycloaddition reaction. Alkynylation and azidation are the main method to modify hydroxyl terminated polyether. Qu et al.[17] synthesized alkyne terminated polyethylene glycol via nucleophilic substitution reaction between polyethylene glycol (PEG) and propargyl bromide. Reshmi et al.[18] employed the same reaction to get propargyloxy terminated polytetramethylene oxide (PTMP). This pre-polymer cured using GAP as an azide bearing polymer and the resultant crosslinked network copolymer provides superior processability and improved ballistic properties in terms of large amount of gas generating species during combustion. Zhang et al.[19] synthesized azido terminated polyethylene glycol by halogenating reaction and azidation two-step method. And more significantly, the modifier gives a lower glass-transition temperature than parent polymer. They also applied the same method to get azide terminated ethylene oxide-tetrahydrofuran random copolymer.[20] Zhai et al.[21] prepared a kind of elastomer based on ATPET by employing tripropargylamine as a curing agent and give the precise network model of the elastomer on various functional molar ratios. Furthermore, the polytriazoles polymers with the urethane segments has been reported by Li et al.[15a] According to Li et al., the urethane segments can effectively improve the mechanical properties of the resultant polytriazoles and it is because that the enhanced intermolecular interaction can benefit for the hard domains aggregation and microphase separation comparing to the pure polytriazoles systerms.

All of aboved-mentioned inspired us to employ a facile method to combine triazole and urethane in one networks. To date, few studies regarding the elastomer based on polyether containing both triazole and urethane can be available. Meanwhile, traditional modified method employing isocyanates like TDI[2,15a] or MDI[22] will produce a solid prepolymer with unavoidable side reaction in preparation and poor processability in application. In this paper, we firstly synthesized a liquid prepolymer azide terminated ethylene oxide-tetrahydrofuran copolymer with urethane segments (ATUPET) via a simple one-pot procedure with a high yield. The terminal azide in the telechelic pre-polymer is expected to cured by acetylene curing agent via 1,3-dipolar cycloaddition reaction. And the pre-existing urethane segment is also designed to enhance intermolecular hydrogen bond interaction and merit the mechanical properties of the resultant elastomer.

2. Results and Discussion

2.1. Structure Characterization

The FTIR spectra for PET, ClTUPET and ATUPET are shown in Figure 1. The spectrum of PET shows the characteristic broad stretching frequency at around 3484 cm^{-1} is due to terminal OH of HTPE and it also indicates a strong intermolecular hydrogen bonding between the OH groups of different polymer chains exists. The bands around 2939 and 2861 cm^{-1} explains the C–H anti-symmetric and symmetric stretch vibration of PET while the peak at 1356 cm^{-1} accounts for the C–H deformation vibration. The strong absorption peak at 1115 cm^{-1} is attributed for the –C–O–C– of PET. Comparatively, the spectrum of ClTUPET shows similar major characteristic vibration peaks at 2940, 2861, 1356 and 1114 cm^{-1} which reveal an unchanged main chain structure. Meanwhile, the peak of the hydroxyl groups disappears in the ClTUPET spectrum. Additionally, new peaks around at 3510 and 3330 cm^{-1} are attributed to the stretching frequency of –NH related to hydrogen bonding[23] and the new strong peak at 1725 cm^{-1} is assigned to –C=O in urethane. When compared ATUPET with PET and ClTUPET, the FTIR of ATUPET also shows an unchanged chain structure. More significantly, appearance of a new stretching band for C–N_3 at 2100 cm^{-1} indicates a successful azide reaction. It is worth to be noted that the weak signal peak around at 746 cm^{-1} due to the –C–Cl of ClTUPET is covered by the aliphatic ether main chain structure.

The ^1H NMR spectra for PET, ClTUPET and ATUPET are shown in Figure 2. Three similar spectra mean a similar main chain structure between them. In the PET spectrum, the single peak at around 1.6 ppm and multiple peaks at approximately 3.2 ~ 3.8 ppm are major typical peaks of hydrogen atoms. The former is clearly attributed to the four methylene protons in the middle of the tetrahydrofuran segment (–$OCH_2CH_2CH_2CH_2$–) and the latter are assigned to the four protons in the methylene connected to ether group in the ethylene glycol segment and tetrahydrofuran segment (–OCH_2CH_2–, –$OCH_2CH_2CH_2CH_2$–). In the ClTUPET and ATUPET spectra, there are two new peaks at around 4.2 ppm and 5.3 ppm, respectively. The relationship between two peak area integral is closed to 2 : 1. Therefore, the

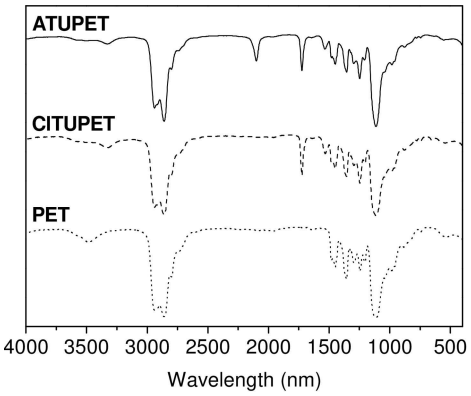

Figure 1. FTIR spectra for PET, ClTUPET and ATUPET.

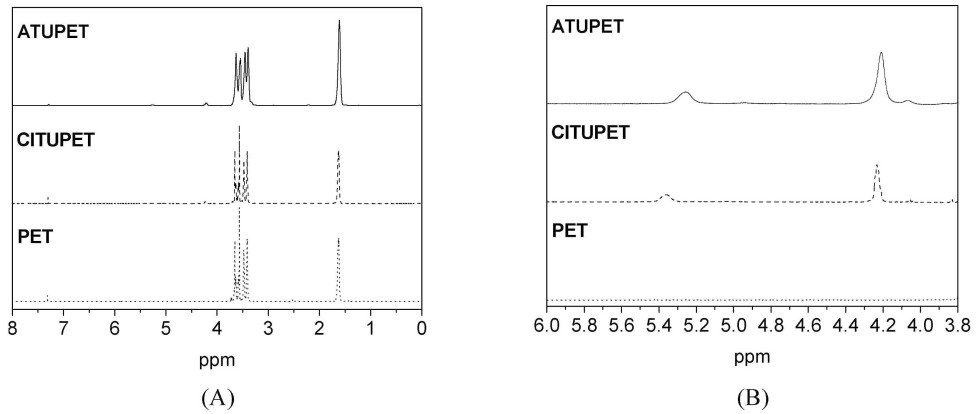

Figure 2. [1]H NMR spectra of (A) PET, CITUPET and ATUPET; (B) local magnification from 6.0 ~ 3.8 ppm.

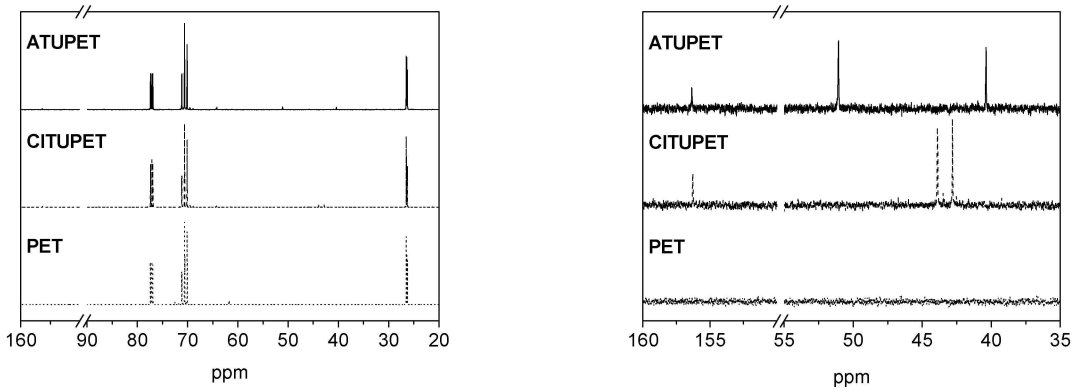

Figure 3. [13]C NMR spectra of (A) PET, CITUPET and ATUPET; (B) local magnification from 150 ~ 160 ppm and 35 ~ 55 ppm.

peak at around 4.2 ppm can be attributed to the terminal protons in the methylene connected ester group (–CH_2–O–CO–$NHCH_2CH_2Cl$, –CH_2–O–CO–$NHCH_2CH_2N_3$) while the peaks at approximately 5.3 ppm can be attributed to protons in urethane (–CH_2–O–CO–$NHCH_2CH_2Cl$, –CH_2–O–CO–$NHCH_2CH_2N_3$). Additionally, the methylene protons in end-capped groups are covered by the multiple peaks at 3.3 ~ 3.6 ppm.

The [13]C NMR spectra for PET, CITUPET and ATUPET are shown in Figure 3. In the PET spectrum, carbon atoms associated with the hydroxyl group in glycol unit and tetrahydrofuran unit are clearly attributed to 61.75 and 61.68 ppm, respectively. In the [13]C NMR spectrum of CITUPET, the new peak around at 156.27 ppm accounts for the –C=O in the new urethane. Because the terminal hydroxyl group was replaced by 2-chloroethyl via urethane, the two peaks at 61.75 and 61.68 ppm that are attributed to the primary carbon atoms associated with hydroxyl group completely disappear and moved to around at 64.28 and 64.19 ppm. Additionally, the two peaks at 43.88 and 42.79 ppm are originated from the α-CH_2 and β-CH_2 connected to terminal –Cl, respectively. After azidation, these two peaks disappear in the [13]C NMR spectra of ATUPET and the new peaks at 51.06 ppm and 40.37 ppm are attributed to the α-CH_2 and β-CH_2 connected to terminal –N_3. Furthermore, the peak around at 156.35 ppm apparently accounts for the –C=O in the urethane of ATUPET.

The GPC traces and their corresponding parameters of PET and ATUPET are shown in Figure 4 and listed in Table 1,

Table 1. The parameters of prepolymer PET and ATUPET.

	M_n	M_w	M_z	PDI
PET	4.93×10^3	7.24×10^3	9.24×10^3	1.47
ATPET	5.37×10^3	7.73×10^3	9.73×10^3	1.44

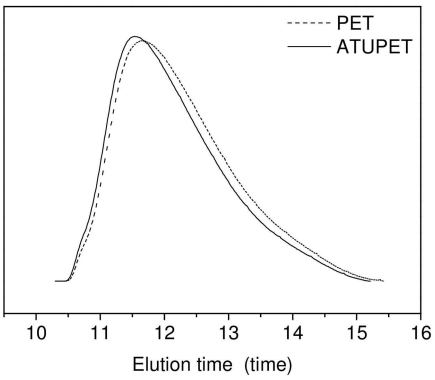

Figure 4. GPC curves of prepolymer PET and ATUPET.

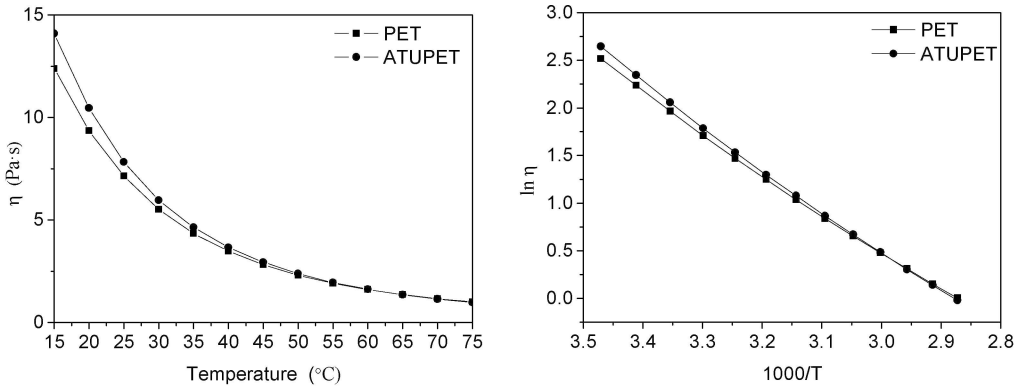

Figure 5. Dependence of viscosity on temperature for PET and ATUPET.

respectively. It can be seen that the two traces are notably similar. The number average molecular weight (M_n) of ATUPET is 5.37×10^3 g mol^{-1}, which is slightly higher than the M_n value of PET (4.93×10^3 g mol^{-1}). Moreover, the polydispersity index between the two pre-polymers do not change significantly. These results suggest that few side reactions like chain extensions and break reactions occur during the preparation process. Furthermore, the prepolymer ATUPET has been synthesized from PET only through end-modification.

Azide value is one of the key parameters for ATUPET in the preparation of elastomer. Hence, it is necessary to give it a quantitative description. Assuming that all of the terminal hydroxyls has been converted into azides, the theoretical azide content of ATUPET is evaluated as 0.446 mmol g^{-1} according to Eq.(1).

$$C_{azide} = C_{hydroxyl}/(1 + C_{hydroxyl} \times 112) \quad (1)$$

where C_{azide} is the content of azide (mmol g^{-1}), $C_{hydroxyl}$ is the hydroxyl content of PET (0.470 mmol g^{-1}).

ATUPET can be simplified to be made up of three units such as tetrahydrofuran chain segments (T, –$OCH_2CH_2CH_2CH_2$–), ethylene glycol chain segments (E, –OCH_2CH_2–) and azide isocyanatoethane terminal segments (I, OCN–$CH_2CH_2N_3$). Furthermore, there is a stoichiometric relationship between the integral area and the mole value of a given structure segment. Therefore, the experimental azide content can be evaluated via ^{1}H NMR. Because the nitrogen of ATUPET is only from the azide group and urethane segment, the experimental azide content of ATUPET is evaluated as 0.449 mmol g^{-1} according to Eq.(2), which is notably close to the theoretical value of 0.446 mmol g^{-1}.

$$C_{azide} = 1/(M_T \times N_T + M_E \times N_E + M_I \times N_I) = 1/(M_T \times 0.5S_T + M_E \times 0.5S_E + M_I \times S_I) \quad (2)$$

where C_{azide} is the mole content of azide (mmol g^{-1}), M_T, M_E and M_I are the molecular weight of specific structures in the accordance with tetrahydrofuran chain segments, ethylene glycol chain segments and azide isocyanatoethane terminal segments. N_T, N_E and N_I are the mole values of the above-mentioned three segments, respectively. S_T, S_E and S_I are the integral areas of the corresponding protons.

2.1.1. Viscosity

The viscositiy of the pre-polymer is an important parameter for the processiblity of propellant. The pre-polymer with proper viscosity will give propellant slurry a good flowability and it is also beneficial to the casting process. The dependences of viscosities on temperature for PET and ATUPET are shown in Figure 5. It can be seen that the viscosities of both PET and ATUPET rapidly decrease with the increase in temperature from 25 °C to 75 °C, giving good exponential relationship as general other polymer.

Furthermore, the exponential relationship between the viscosity and thermodynamic temperature follows the Andrade equation (Eq. 3) and its logarithmic equation can be shown as Eq. 4:

$$\eta = Ae^{\Delta E\eta/RT} \quad (3)$$

$$\ln\eta = \ln A + \Delta E_\eta/RT \quad (4)$$

where η is the viscosity of the polymer, A is a constant, R is the gas constant, T is thermodynamic temperature and ΔE_η is the flow-activation energy of the polymer. Generally, the flow-activation energy (ΔE_η) is the energy needed to overcome the interaction of surrounding molecules when a molecule transitions to the hole and the ΔE_η value can be used to give a quantitative description about the sensitivity of viscosity to temperature. According to the lnη-1000/T curves shown in Figure 5 (B), the curves display a well linear relationship and the specific ΔE_η value can be evaluated from the slope of the corresponding line. Finally, the detailed dependence of viscosity on temperature is analyzed in Table 2.

Table 2. The dependence of $\triangle E_\eta$ and T.

Sample	η-T	ln η−1000/T	ΔE_η
PET	$y = 200.2\ e^{-0.04x}$ ($R^2 = 0.990$)	$y = 4.194x - 12.10$ ($R^2 = 0.997$)	34.87
ATUPET	$y = 233.9\ e^{-0.04x}$ ($R^2 = 0.990$)	$y = 4.445x - 12.85$ ($R^2 = 0.997$)	36.96

It is also worth to be noted that the modifier has slightly higher viscosities than its parent polymer at the experimental temperature range because of a relatively higher $\triangle E_\eta$ value of ATUPET. Generally, the higher $\triangle E_\eta$ value means the less flexible main chain or the greater intermolecular interaction of the polymer. Obviously, the changes of $\triangle E_\eta$ between PET and ATUPET are mainly because of the hydrogen bonding interaction produced by urethane in ATUPET. Therefore, the viscosity of ATUPET changes a little. But the polymer as a binder prepolymer still has an appropriate flow state in the range of propellant processing temperature.

2.2. Mechanical Properties

The crossed-linked elastomer with 1,2,3-trizole and urethane subunit via click polymerization can be carried out as the method mentioned in the experimental part. The FTIR spectrum of ATUPET based elastomer (R = 1.0) is shown in Supporting Information (Figure S3). In the spectrum of ATUPET based elastomer, the stretching band for C–N_3 at 2100 cm^{-1} as the important typical peak of ATUPET disappeared. Additionally, the disappeared typical peak about the C–H stretching band of the propargyl groups at around 3303 cm^{-1} also can confirm the complete conversion of the ATUPET to its elastomer.

The mechanical properties of polytriazoles elastomers based on ATUPET/tripropargylamine with various R values (S1-S7) are listed in Table 3 and shown in Figure 6. The elastomer modulus

Table 3. Mechanical properties of polytriazoles elastomers.

Sample	R value	Mechanical properties *Modulus, E/ MPa*	*Tensile strength, σ_b/MPa*	*Elongation at the break, ε_b/%*
S1	0.7	0.09	0.41	1434.49
S2	0.8	0.33	0.59	536.72
S3	0.9	1.19	0.95	157.72
S4	1.0	2.27	1.35	111.95
S5	1.1	2.40	1.30	85.05
S6	1.2	2.20	1.21	76.19
S7	1.3	2.09	1.01	71.59

E and tensile strength σ_b first increase from 0.09 and 0.41 MPa to 2.27 and 1.35 MPa and then decrease to 2.09 and 1.01 MPa with increasing R. In contrast, the elongation at the break ε_b decreases from 1434.49% to 71.59% with the R varied from 0.7 to 1.3. The dependence of modulus *E* and tensile strength σ_b on virous R values shown in Figure 6 is clearly parabolic but

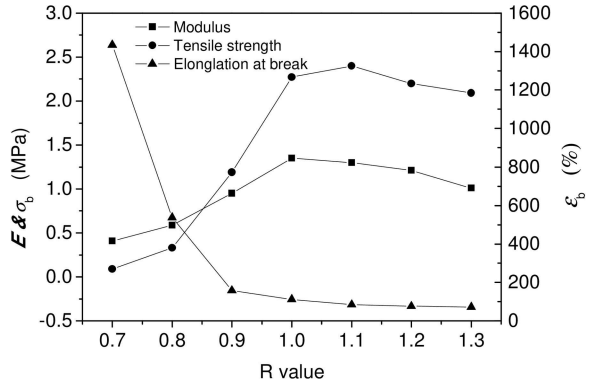

Figure 6. Dependence of mechanical properties on R value for polytriazoles elastomers S1–S7.

asymmetrical and the values of E and σ_b reach to maximum at the stoichiometric ratio (R = 1.0). These tendencies shown are in good agreement with previous report.[17b,21] The rapid decrease of elongation at the break with the R from 0.7 to 1.0 also give the same trend as the previous report. However, the slightly decrease of ε_b values with the R from 1.0 to 1.3 shown in Figure 6 is unexpectedly. This phenomenon will be discussed latter in this paper.

2.3. Network Structure

The volume selling curves of the polytriazoles elastomers are shown in Figure 7. It can be seen that the initial volume swelling rates of elastomers gradually decrease from S1 to S4 and then increase from S4 to S7 slightly. Elastomer S4 with the stoichiometric ratio (R = 1.0) has the smallest volume swelling rate. Additionally, it also can be seen that all volume swelling curves initially rapidly ascend and subsequently slowly increase. After approximately 500 min, all the volume swelling ratios of polytriazoles elastomers reach equilibrium, and the elastomer S4 with the stoichiometric ratio (R = 1.0) has a minimum equilibrium volume swelling ratio.

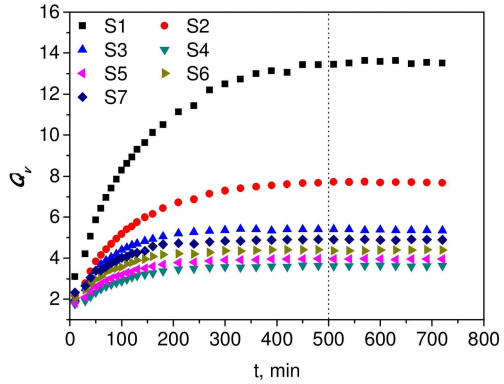

Figure 7. Volume swelling curves of polytriazole selastomers.

Table 4. Structural parameters of ATUPET-based elastomers.

Sample	R value	χ_1	Q_v	v_{2m}	ρ, g cm^{-3}	M_c, g mol^{-1}	N_0, mmol cm^{-3}
S1	0.7	0.383	13.583	0.074	1.053	54728.1	0.019
S2	0.8	0.383	7.686	0.130	1.054	17753.6	0.059
S3	0.9	0.383	5.386	0.186	1.055	8195.6	0.129
S4	1.0	0.383	3.646	0.274	1.056	3299.7	0.320
S5	1.1	0.383	3.958	0.253	1.057	4014.5	0.263
S6	1.2	0.383	4.390	0.228	1.055	5135.8	0.205
S7	1.3	0.383	4.887	0.205	1.055	6575.3	0.160

Based on the equilibrium swelling ratios (Q_v) of polymers, the volume fractions (v_{2m}) in the swollen elastomers can be calculated using Eq. (5). The Flory-Huggins interaction parameter between the polymer and solvent (χ_1) can also be evaluated by the Bristow Watson Equation, Eq. (6).[24] Thus, the apparent number average molecular weights (M_c) of elastomer strands can be further evaluated according to the Flory-Huggins theory (Eq. 7).[25] Furthermore, the apparent cross-linking densities (N_0) also can be determined by Eq. (8).

$$v_{2m} = 1/Q_v \tag{5}$$

$$\chi_1 = 0.34 + V(\delta_S - \delta_P)^2/RT \tag{6}$$

$$M_c = -V\rho\,(v_{2m}^{1/3} - v_{2m}/2)/[\ln(1-v_{2m}) + v_{2m} + \chi_1 v_{2m}^2] \tag{7}$$

$$N_0 = \rho/M_c \tag{8}$$

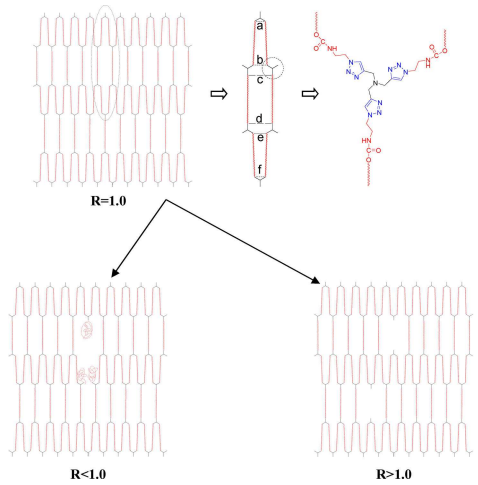

Figure 8. Network model of elastomers based on ATUPET a, b, c, d, e and f refer to the possible hydrogen bond position.

Where V is the molar volume of toluene solvent (106.4 cm^3 mol^{-1}), R is the gas constant, T is the absolute temperature, ρ is the density of the elastomer, δ_S and δ_P are the solubility parameter of the elastomer and the solvent, respectively, which are evaluated to be 19.2 (J cm^{-3})$^{1/2}$ and 18.2 (J cm^{-3})$^{1/2}$. The calculated structural parameters of ATUPET-based elastomers are listed in Table 4.

The calculated structural parameters of ATUPET-based elastomers S1-S7 are listed in Table 4. It can be seen that the apparent number average molecular weights (M_c) of these elastomers initially decreases from 54728.1 g mol^{-1} to the minimum 3299.7 g mol^{-1} at the stoichiometric ratio (R = 1.0) with increasing R. Then M_c value increases slightly to 6575.3 g mol^{-1} with the further increase in R. Likewise, the apparent cross-linking densities (N_0) firstly increases from 0.059 mmol cm^{-3} to the maximum 0.320 mmol cm^{-3} when R is 1.0 and then decreases to 0.160 mmol cm^{-3}.

The network structures of polytriazoles elastomers prepared by Cu(I) catalyzed Huisgen reaction without side reactions are shown schematically in Figure 8. When R is around 1.0, the terminal azide groups of ATUPET can completely react with alkynyl groups of tripropargylamine at stoichiometric ratio. And the resulting network structure composed of several slender hexagon grids is close to perfection. Therefore, M_c is at a minimum and N_0 is at a maximum. It is worth to be noted that each hexagon grid must be thinner than general ones because of the extra hydrogen bonding arised from urethane in ATUPET (Figure 8 R = 1.0 a ~ f). When R < 1.0, the terminal azide groups of ATUPET cannot be completely reacted with alkynyl groups and the excess polymer chains form many dangling strands in the network structure. Consequently, the elastomers exhibit higher M_c and lower N_0. Inversely, when R > 1.0, the alkynyl groups of tripropargylamine cannot be reacted and the surplus alkynyl groups will also append some cross-linking points. This can cause the increase of M_c and the decrease of N_0.

Generally, the tensile strength σ_b and elastomer modulus E of the cross-linked elastomer are proportional to the cross-linking density N_0.[26] Therefore, it can be inferred that σ_b and E of ATUPET-based polytriazoles elastomer first increase to a maximum rapidly and then decrease slightly because of the same tendency of N_0. With regard to the unexpected tendency of the elongation at break ε_b, when R < 1.0, both of the greater apparent average molecular weight M_c[27] and the internal plasticization[28] arised from the excess polymer chains in the grid can benefit the elongation. Consequently, ε_b decreases rapidly with the increasing R from 0.7 to 1.0. However, when R increases from 1.0 to 1.3, the M_c increases slightly and it results in a less influence on ε_b. Meanwhile, the hydrogen bond arised from urethane in network will enhance the intermolecular interaction without the interference of the surplus pre-polymer and it acts as a lock to prevent the chain of molecular from free movement. Additionally, when R > 1.0, the ratio of the soft segments and the hard segments will decrease slightly. It means that the increase of the content of hard segment weaken

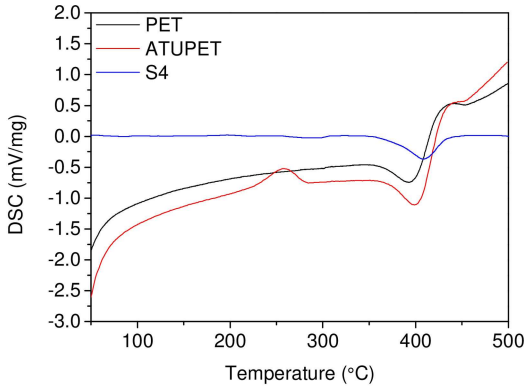

Figure 9. DSC traces of PET, ATUPET and elastomer S4.

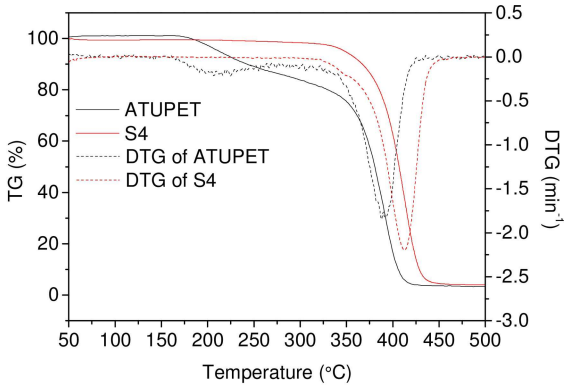

Figure 10. TG and DTG traces of ATUPET and elastomer S4.

the ε_b. Furthermore, the absence of the internal plasticization, the hindrance from hydrogen bonding interaction and the slight increase in the content of hard segment will all worsen the elongation. Therefore, ε_b still decreases unexpectedly when $R > 1.0$, but this trend shows more slight.

2.4. Thermal Properties

The thermal stability of energetic materials and their additives plays an important role in their preparation, processing, storage, and application.[29] Therefore, the thermal decomposition behaviors of PET, ATUPET and the resultant polytriazoles S4 were studied using DSC methods. As shown in Figure 9, the DSC curve of PET presents a main single endothermic event with maximum at around 400 °C. And it is consistent with the reports about the major endothermic one of hydroxyl-terminated polyether prepolymers in Refs.[30] Comparatively, the typical DSC curve of ATUPET shows the new exothermic event with maximum at around 250 °C that can be associated with the decomposition of the azide groups to nitrogen molecules.[29c,31] Furthermore, the DSC curve of polytriazoles elastomer (S4) has a one endothermic peak with a maximum at around 400 °C. Considering the decomposition at 570 °C of triazole cross-linking point,[32] it is attributed to the decomposition of polyether chains obviously.

TGA of ATUPET was also applied to study its mass change during thermal decomposition. It can be seen from Figure 10 that the TGA curve of ATUPET shows a continuous two-stage thermal decomposition process. Characteristic first step weight loss temperature at 250 °C is corresponded to the stripping of terminal azide groups from the polyether main chain of PET. And the second main weight loss at around 400 °C was due to the thermal decomposition of PET. It is also can be seen that the second stage was much more sharp with nearly 80% weight loss occur at this stage because of high content polyether backbone in ATUPET. Comparatively, the polytriazoles elastomer S4 just displays a single-stage thermal decomposition process and almost more than 95% weight loss occur at this stage because of high content of polyether and a higher decompostion temperature of triazole in solid elastomer. Anyway, both DSC and TGA confirm that the ATUPET as a modifier and the polytriazoles as a resultant elastomer start to decompose/degrade at high temperature (> 200 °C), thus showing a satisfactory thermal stability.

3. Conclusions

An azide terminated ethylene oxide-tetrahydrofuran copolymer with urethane segments (ATUPET) has been prepared through ethylene oxide-tetrahydrofuran random copolymer (PET) end-capping modification via one-pot method. Consequently, ATUPET has a slightly higher viscosity in comparison with PET because of the additional hydrogen bonding interaction generated by the urethane in ATUPET. Triazole cross-linked elastomers based on ATUPET with various functional molar ratios also have been prepared using tripropargylamine as a curing agent and cross-linker. Mechanical properties show that the modulus E and tensile strength σ_b exhibit a parabolic dependence with the increase in R. At around the stoichiometric ratio, the modulus E and tensile strength σ_b reach a maximum and the elongation at break exhibit an acceptable value at the same time. Additionally, the apparent cross-linking densities (N_0) have a maximum value at the stoichiometric ratio. Thermal analysis shows that the ATUPET prepolymer and its polytriazoles elastomers exhibit a different process in thermal decomposition. ATUPET shows a continuous two-stage thermal decomposition process while the first step weight loss temperature at 250 °C is corresponded to the stripping of terminal azide groups from the polyether main chain of PET and the second main weight loss at around 400 °C is due to the thermal decomposition of PET. Comparatively, ATUPET based elastomer is characteristic of the one-step decomposition with a maximum at around 400 °C because of a higher decompostion temperature of triazole in solid elastomer. These results indicates that ATUPET exhibits good mechanical properties and stability and might serve as a potential binder in propellant formulations especially in the field of isocyanate-free curing technology.

Experimental

Materials

All commercially obtained materials were used without further purification. Ethylene oxide-tetrahydrofuran random copolymer (PET, hydroxyl value of 26.35 mgKOH g^{-1}) was purchased from Liming Research Institute of Chemical Industry (China). PET is colorless transparent viscous liquid. 2-Chloroethyl isocyanate and tripropargylamine were analytical grade commercial products obtained from J&K Scientific (China). Tetrakis(acetonitrile)copper(I) hexafluorophosph (purity 99%) was provided from TCI Shanghai (China). Sodium azide, dibutyltin dilaurate (DBTDL), N,N-dimethylformamide (DMF) and other solvents of high purity (AR grade) were procured from Chengdu Kelong Chemical Reagents Company.

ATUPET Preparation

Chloro-terminated ethylene oxide-tetrahydrofuran copolymer with urethane segments (ClTUPET): PET (63.87 g, 15 mmol) and 2-chloroethyl isocyanate (6.33 g, 60 mmol) were charged into a 100 mL three-necked flask. The reaction was carried out in bulk in the presence of DBTDL as catalyst at 90 °C for 18 h under mechanical stirring, then excess 2- chloroethyl isocyanate was removed at 90 °C in vacuum for 1 h. Finally, the ClTUPET in a yellow oily liquid state was obtained. Yield: 66.95 g (99.87%).

Azide terminated ethylene oxide-tetrahydrofuran copolymer with urethane segments (ATUPET): ClTUPET (58.10 g, 13 mmol) was dissolved in 50 mL DMF in a 100 mL three-necked flask. Sodium azide (NaN_3) (5.07 g, 78 mmol) was then added, and the reaction was carried out with mechanical stirring in an oil bath at 90 °C for 72 h. Subsequently, the solvent DMF was removed from the mixture by rotary evaporation at 80 °C and about 500 mL CH_2Cl_2 was added. Then, the mixture was successively washed thrice with 200 mL distilled water in each occasion. The organic layer was separated and evaporated in vacuum to achieve the target product ATUPET in a yellow oily liquid state. Yield: 53.54 g (92.42%). The synthesis route of ATUPET is shown in Figure 11.

Elastomer Preparation

ATUPET was cured using tripropargylamine via tetrakis(acetonitrile) copper(I) hexafluorophosph as a catalyst. The ATUPET-based elastomer compositions are listed in Table 5. The R value is the equivalent ratio of the tripropargylamine cross-linker alkynyl group to the ATUPET azide group. All the component were stirred thoroughly and degassed in vacuum. The uniform mixtures were then casted in moulds and cured at 50 °C for 5 days. The end-crosslinked elastomers containing both triazole and urethane under ambient condition were obtained.

Table 5. Elastomer components in mass ratio.

sample	R	Catalyst	ATUPET	Tripropargylamine
S1	0.7	0.0772	15.5	0.2134
S2	0.8	0.0772	15.5	0.2435
S3	0.9	0.0772	15.5	0.2744
S4	1.0	0.0772	15.5	0.3045
S5	1.1	0.0772	15.5	0.3343
S6	1.2	0.0772	15.5	0.3658
S7	1.3	0.0772	15.5	0.3966

Swelling Test

Swelling measurements were carried out in toluene at 25 °C. The elastomer specimens were cut into similar sizes (about 0.15 g, 10 × 5 × 2 mm^3 dimensions) and immersed in toluene for special time. Then, the swollen gels were removed from the solvent, quickly blotted with dry filter paper, and weighed until the mass change was less than 0.01 g over a period of 30 min. The equilibrium swelling ratio (Q_v) of the elastomers can be calculated using Eq.(1).[33]

$$Q_v = 1 + (\omega/\omega_0 - 1)\rho_2/\rho_1 \quad (9)$$

where ω_0 and ω is the weight of the un-swollen and swollen specimens, and ρ_1 and ρ_2 are the densities of the solvent and the polymers, respectively.

Characterization

^1H NMR,^{13}C NMR were obtained on a BRUKER AV500 NMR spectrometer, using $CDCl_3$ as the reference solvent. Chemical shifts were reported as parts per million downfield from tetramethylsilane (TMS). Fourier transform infrared (FTIR) spectra were recorded on a BRUKER TENSOR27 infrared spectrometer in the range of 400 ~ 4000 cm^{-1} using KBr plates. GPC measurement were performed with a Waters GPC instrument equipped with Ultra-styragel columns (10, 50, 100 and 1000 nm), a refractive index detector and Datamodule 730. Tetrahydrafuran was used as the mobile phase at a flow rate of 0.8 mL/min through the columns at 30 °C. A series of PS standards were used to generate a GPC calibration curve. Viscosity measurement were performed using a BROOKFIELD CAP 2000 + viscometer with a 20 mm parallel plate geometry, a gap size 1 mm and a rotate speed range from 5-999 RPM. Tensile testing was performed on SHIMADZU EZ-LX universal testing machine with a cross-head speed of 50 mm min^{-1}. The thermal gravimetric analysis (TGA) was performed on the NETZSCH STA 449 thermal analyzer under nitrogen atmosphere at a heating rate of 5 K min^{-1} from 30 °C to 500 °C. The samples of 4 mg were used, and the gas flow rate was 60 mL min^{-1}. The differential scanning calorimetry analyses (DSC) were performed from a NETZSCH DCS 200 F3 differential scanning calorimeter with a heating rate of 10 °C min^{-1} and a gas flow rate was 60 mL min^{-1}.

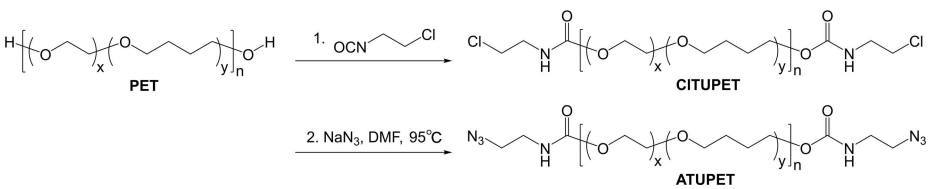

Figure 11. Synthesis route of ATUPET.

Acknowledgements

This work was sponsored by the National Natural Science Foundation of China (No. 21703168).

Conflict of Interest

The authors declare no conflict of interest.

Keywords: ATUPET · 1,3-Dipolar cycloaddition reactions · elastomer · thermal behavior · mechanical properties

[1] Z. S. Petrović, J. Ferguson, *Prog. Polym. Sci.* **1991**, *16*, 695–836.
[2] S. Reshmi, E. Arunan, C. P. R. Nair, *Ind. Eng. Chem. Res.* **2014**, *53*, 16612–16620.
[3] a) K. Menke, T. Heintz, W. Schweikert, T. Keicher, H. Krause, *Propellants Explos. Pyrotech.* **2009**, *34*, 218–230; b) T. Keicher, W. Kuglstatter, S. Eisele, T. Wetzel, H. Krause, *Propellants Explos. Pyrotech.* **2009**, *34*, 210–217; c) D.-H. Lee, K. T. Kim, Y. Jang, S. Lee, H. B. Jeon, H.-j. Paik, B. S. Min, W. Kim, *J. Appl. Polym. Sci.* **2014**, *131*.
[4] T. Huimin, *The Chemistry and Technology of Solid Rocket Propellant*, Beijing Institute of Technology Press, **2015**.
[5] N. Li, X. Gan, H. Mo, L. Li, X. Lu, T. Han, *Chinese Journal of Energetic Materials* **2011**, *19*, 505–508.
[6] W. H. Binder, R. Sachsenhofer, *Macromol. Rapid. Commun.* **2007**, *28*, 15–54.
[7] A. Gandini, D. Coelho, M. Gomes, B. Reis, A. Silvestre, *J. Mater. Chem.* **2009**, *19*, 8656–8664.
[8] J. P. Swanson, S. Rozvadovsky, J. E. Seppala, M. E. Mackay, R. E. Jensen, P. J. Costanzo, *Macromolecules* **2010**, *43*, 6135–6141.
[9] a) R. Huisgen, *Angew. Chem. Int. Ed.* **1963**, *2*, 633–645; *Angew. Chem.* **1963**, *75*, 742–754; b) R. A. Firestone, *J. Org. Chem.* **1968**, *33*, 2285–2290; c) V. V. Rostovtsev, L. G. Green, V. V. Fokin, K. B. Sharpless, *Angew. Chem. Int. Ed.* **2002**, *41*, 2596–2599; *Angew. Chem.* **2002**, *114*, 2708–2711; d) S. Binauld, D. Damiron, T. Hamaide, J.-P. Pascault, E. Fleury, E. Drockenmuller, *Chem. Commun.* **2008**, 4138–4140; e) N. V. Tsarevsky, S. A. Bencherif, K. Matyjaszewski, *Macromolecules* **2007**, *40*, 4439–4445; f) D. Döhler, P. Michael, W. H. Binder, *Macromolecules* **2012**, *45*, 3335–3345.
[10] a) F. Himo, T. Lovell, R. Hilgraf, V. V. Rostovtsev, L. Noodleman, K. B. Sharpless, V. V. Fokin, *J. Am. Chem. Soc.* **2005**, *127*, 210–216; b) P. Wu, A. K. Feldman, A. K. Nugent, C. J. Hawker, A. Scheel, B. Voit, J. Pyun, J. M. J. Fréchet, K. B. Sharpless, V. V. Fokin, *Angew. Chem. Int. Ed.* **2004**, *43*, 3928–3932; *Angew. Chem.* **2004**, *116*, 4018–4022; c) R. Huisgen, *Angew. Chem. Int. Ed.* **1963**, *2*, 565–598; *Angew. Chem.* **1963**, *75*, 604–637.
[11] a) C. Hu, X. Guo, Y. Jing, J. Chen, C. Zhang, J. Huang, *J. Appl. Polym. Sci.* **2014**, *131*; b) B. S. Min, Y. C. Park, J. C. Yoo, *Propellants Explos. Pyrotech.* **2012**, *37*, 59–68; c) S. K. Reshmi, K. P. Vijayalakshmi, D. Thomas, E. Arunan, C. P. Reghunadhan Nair, *Propellants Explos. Pyrotech.* **2013**, *38*, 525–532.
[12] N. Li, F. Zhao, Y. Luo, H. Mo, H. Gao, L. Xiao, E. Yao, R. Hu, *Propellants Explos. Pyrotech.* **2015**, *40*, 808–813.
[13] A. Tanver, M.-H. Huang, Y. Luo, *RSC Adv.* **2016**, *6*, 49101–49112.
[14] G. V. Malkov, A. V. Shastin, Y. I. Estrin, E. R. Badamshina, Y. M. Mikhailov, *Propellants Explos. Pyrotech.* **2008**, *33*, 431–436.
[15] a) H. Li, Q. Yu, F. Zhao, B. Wang, N. Li, *J. Appl. Polym. Sci.* **2017**, *134*, 45178; b) Y. Ding, C. Hu, X. Guo, Y. Che, J. Huang, *J. Appl. Polym. Sci.* **2013**, *131*; c) S. Reshmi, K. P. Vijayalakshmi, D. Thomas, R. Rajeev, C. P. Reghunadhan Nair, *Combust. Flame* **2016**, *167*, 380–391; d) J. Dong, R. Yang, J. Zhai, *Polym. Mater. Sci. Eng.* **2015**, *31*, 6–10.
[16] D.-H. Lee, K. T. Kim, H. Jung, S. H. Kim, S. Park, H. B. Jeon, H.-j. Paik, B. S. Min, W. Kim, *Journal of the Taiwan Institute of Chemical Engineers* **2014**, *45*, 3110–3116.
[17] a) Z. Qu, J. Zhai, H. Zhang, R. Yang, *Chin. J. Explos. Propellants* **2010**, *33*, 61–64; b) Z. Qu, J. Zhai, R. Yang, *Polym. Adv. Technol.* **2014**, *25*, 314–321.
[18] S. Reshmi, H. Hemanth, S. Gayathri, C. P. Reghunadhan Nair, *Polymer* **2016**, *92*, 201–209.
[19] H. Zhang, J. Zhai, Z. Qu, R. Yang, *Chin. J. Explos. Propellants* **2011**, *34*, 45–47.
[20] H. Zhang, J. Zhai, R. Yang, *Chin. J. Explos. Propellants* **2012**, *35*, 45–48.
[21] J. Zhai, N. Zhang, X. Guo, J. He, D. Li, R. Yang, *Eur. Polym. J.* **2016**, *78*, 72–81.
[22] G. Wang, S. Guo, Y. Ding, *Macromol. Chem. Phys.* **2015**, *216*, 1894–1904.
[23] a) J. Mattia, P. Painter, *Macromolecules* **2007**, *40*, 1546–1554; b) G. Wang, Y. Luo, *Propellants Explos. Pyrotech.* **2016**, *41*, 850–854; c) C. Zhang, Z. Ren, Z. Yin, H. Qian, D. Ma, *Polym. Bull.* **2008**, *60*, 97–101.
[24] G. M. Bristow, W. F. Watson, *Trans. Faraday Soc.* **1958**, *54*, 1742–1747.
[25] P. J. Flory, J. Rehner, *J. Chem. Phys.* **1943**, *11*, 521–526.
[26] D. J. Hourston, Y. Zia, *J. Appl. Polym. Sci.* **1983**, *28*, 2139–2149.
[27] K. Urayama, T. Kawamura, S. Kohjiya, *Polymer* **2009**, *50*, 347–356.
[28] a) P. Jia, L. Hu, Q. Shang, R. Wang, M. Zhang, Y. Zhou, *ACS Sustainable Chem. Eng.* **2017**, *5*, 6665–6673; b) C. M. Higa, A. T. Tek, R. J. Wojtecki, R. Braslau, *J. Polym. Sci. Part A* **2018**, *56*, 2397–2411; c) C. B. Ciulik, O. D. Bernardinelli, D. T. Balogh, E. R. de Azevedo, L. Akcelrud, *Polymer* **2014**, *55*, 2645–2651.
[29] a) H. Abusaidi, H. R. Ghaieni, *J. Therm. Anal. Calorim.* **2016**, 1–6; b) Q. Wang, L. Wang, X. Zhang, Z. Mi, *J. Hazard. Mater.* **2009**, *172*, 1659–1664; c) M. Xu, Z. Ge, X. Lu, H. Mo, Y. Ji, H. Hu, *RSC Adv.* **2017**, *7*, 47271–47278.
[30] a) J.-O. Kweon, Y.-K. Lee, S.-T. Noh, *J. Polym. Sci. Part A* **2001**, *39*, 4129–4138; b) D. K. Chattopadhyay, D. C. Webster, *Prog. Polym. Sci.* **2009**, *34*, 1068–1133; c) K. Mao, M. Xia, Y. Luo, *J. Elastomers Plast.* **2015**, *48*, 546–560.
[31] M. Xu, Z. Ge, X. Lu, H. Mo, Y. Ji, H. Hu, *Polym. Int.* **2017**, *66*, 1318–1323.
[32] a) Y. Tang, C. K. W. Jim, Y. Liu, L. Ye, A. Qin, J. W. Y. Lam, C. Zhao, B. Z. Tang, *ACS Appl. Mater. Interfaces* **2010**, *2*, 566–574; b) A. Qin, C. K. W. Jim, W. Lu, J. W. Y. Lam, M. Häussler, Y. Dong, H. H. Y. Sung, I. D. Williams, G. K. L. Wong, B. Z. Tang, *Macromolecules* **2007**, *40*, 2308–2317.
[33] H. Li, F. Zhao, Q. Yu, B. Wang, X. Lu, *J. Appl. Polym. Sci.* **2016**, *133*.

Manuscript received: February 18, 2019
Revised manuscript received: March 19, 2019

